

Uniform multiple laminates interpolation method for angle optimization of Double-Double composite laminates based on multi-material topology optimization strategy

FANG Pingchu¹, WANG Dan², GAO Tong¹*, HUANG Yongbin¹, SONG Longlong¹, DUYSINX, Pierre³, ZHANG Weihong

¹ State IJR Center of Aerospace Design and Additive Manufacturing, School of Mechanical Engineering, Northwestern Polytechnical University, Xi'an, 710072, China

² Institute of High Performance Computing (IHPC), Agency for Science, Technology and Research (A*STAR), 1 Fusionopolis Way, #16-16 Connexis, 138632, Republic of Singapore

³ Aerospace and Mechanical Engineering, University of Liege, Belgium

Abstract

Double-Double (DD) laminates present an innovative laminate layup, incorporating a repetition of sub-plyes featuring two groups of balanced angles. This layup provides composite materials a broad design flexibility together with the ease of design and manufacturing. In this work, an optimization design method is proposed for DD laminates based on multi-material topology optimization. The uniform multiple laminates interpolation (UMLI) model is proposed to describe the certainty of the stacking direction in multi-layer composite structures, inspired by the interpolation model in multi-material topology optimization. Specifically, the stiffness matrices of all alternative angle combinations of DD laminates are interpolated to form virtual laminates. The UMLI model significantly reduces the number of design variables for each individual element and eliminates the need for adding interlayer constraints during optimization. The optimization problem is defined to minimize the compliance of the composite structures and is solved using the gradient-based optimization algorithm. Finally, the method was applied to the design of composite stiffened panels and the wing of a composite Unmanned Aerial Vehicle (UAV). The optimal results demonstrate that the optimized DD laminates exhibit superior performance compared to Quad laminates.

Keyword: Composite materials, Double-double laminates, multi-material topology optimization, discrete material, the uniform multiple laminates interpolation

1. Introduction

Composite materials are typically manufactured as fiber-reinforced laminate structures, widely used in aerospace and other high-performance applications due to their exceptional specific strength and stiffness^{1,2}. The properties of composite laminates, including stiffness, strength, and buckling behavior, are closely linked to the fiber orientation and lamination thickness. As such, optimizing the fiber angle design has become a highly sought-after objective in the structural design of composite laminates to achieve superior performance.

Composite laminates optimization design encompasses two primary approaches: heuristic algorithm and gradient algorithm. Heuristic methods, which do not require gradient information

of optimization problems, have the capacity to discover the global solution. Genetic algorithm (GA)³, simulated annealing (SA)^{4,5}, particle swarm optimization algorithm (PSO)^{6,7}, and other heuristic algorithms have been successfully applied to optimizing various responses of composite laminates, including weight⁸, buckling load⁹, stiffness¹⁰, fundamental frequency¹¹, and others. Moreover, there are scholars¹² who incorporate constraints of composite manufacturing processes into genetic algorithms for optimal design of composite structures. Nevertheless, heuristic algorithms often encounter challenges such as exorbitant computational demand, difficulties in convergence, and inefficiency. Gradient algorithm is also employed in the optimization of composite materials, owing to its advantage of high solving efficiency. Nevertheless, the gradient algorithm typically yields a local solution, and it can be challenging to discover the global optimum. Additionally, obtaining gradient information can be difficult, necessitating the utilization of difference methods or approximation techniques¹³. Common optimization algorithms used include Optimality Criterion Method (OC), Method of Moving Asymptotes (MMA), Generalized MMA (GMMMA), The globally convergent version of MMA (GCMMA), CONLIN, the method of diagonal quadratic approximation (MDQA)^{14,15,16} etc. In optimization problems of composite structures, the design variables typically consist of the ply thickness and ply angle of composite materials, and the objective functions include composite stiffness, fundamental frequency, buckling, weight^{17,18,19} etc.

The alternative angles of composite laminates are typically discrete rather than continuous. Consequently, the angle optimization problem of composite structures can reformulated as a multi-material topology optimization problem where each alternative angle is regarded as an independent material. The uniform multiphase materials interpolation (UMMI) scheme²⁰ which is known as discrete material optimization (DMO) and firstly proposed by Stegmann and Lund²¹, is a typical method. The UMMI approach can converge to one of the alternative angles for each element by penalizing the intermediate elemental angles which are interpolated from the alternative angles with equal weights ranging from 0 to 1. The results demonstrate that this method can be applied to stiffness optimization design²², natural frequency optimization design²³, and local dynamic response of composite materials²⁴.

Subsequently, several similar discrete material interpolation methods have also been further developed. Bruyneel²⁵ proposed a new parametric method for material optimization: Shape function and penalty (SFP). This approach reduced the number of design variables by employing the representation of shape functions. Gao et al.²⁶ proposed the bi-value coding parameterization (BCP) method, which can use n design variables to represent a maximum of 2^n alternative angles, greatly reducing the number of design variables. This method is therefore better equipped to handle optimization problems involving composite materials with a large number of alternative angles. Luo et al.²⁷ proposed the discrete-continuous parameterization (DCP) method, which determined the value subinterval of fiber angle through discrete angle, and then used continuous optimization to determine fiber angle from the subinterval, thereby avoiding the occurrence of local solutions to a certain extent. Zhang et al.²⁸ proposed the bipartite interpolation optimization method (BIO), which can use n design variables to represent a maximum of 2^n alternative angles, reducing the design variables. In addition, some scholars have considered manufacturing constraints when using multi-material topology optimization methods to optimize composite laminates. Yan et al.²⁹ incorporated adjacent constraints, 10% constraints, equilibrium constraints, damage tolerance constraints and symmetric constraints into the

optimization problem, and adopted the sequential linear programming optimization algorithm with mobility constraints to solve the problem.

However, optimization design of composite ply angles in practical engineering remains a challenging task due to the constraints imposed by the manufacturing process. The main design constraints^{30,31,32,33,34,35} are as follows:

- (a) Symmetry constraint: The fiber angles of laminates are usually stacked in a symmetrical order in order to reduce the warping caused by tension-bending coupling.
- (b) Balance Constraint: To mitigate tension-shear coupling, laminates are designed with an equal number of fiber angles in opposite orientations.
- (c) Minimum Percentage Constraint: Each ply angle orientations must remain a minimum proportion, typically 10%, of the total number of stacked plies to avoid stratification of laminates.
- (d) Continuity Constraint: The number of blocked plies with the same angle orientation must be limited to prevent crack propagation in laminates.

Double-double (DD) laminates proposed by Tsai³⁶ provide a fresh and innovative solution by incorporating a repetition of sub-ply layers featuring two groups of balanced angles. Due to its special stacking sequence, DD laminates yield more homogenized bending properties compared to the conventional Quad laminates, which only includes 0, ± 45 , and 90 degree angles. Simultaneously, DD laminate meet most of the above-mentioned design constraints in stacking direction, while keeping the simplicity of a four plies of sub-ply layers. Moreover, DD laminates can provide a lightweight design for easy tapering. All these advantages of DD laminates attract the attention of many researchers from both academic and industry.

Shrivastava et al.³⁷ used artificial intelligence genetic algorithm to optimize the wing quality of DD laminates by considering unit-circle failure, buckling mode and wing-tip deflection design criteria. Zhao et al.³⁸ proposed a new formula for calculating the lamination parameters of DD laminates. On this basis, the feasible region of any combination of two lamination parameters is obtained by using Lagrange multiplier analysis. Vermes et al.³⁹ proposed the lamination method and advantages of DD laminates. The DD lamination method can significantly reduce the number of plies required for laminates, thereby reducing the weight of the composite structure. Kappel et al.⁴⁰ proposed an optimization method based on failure envelope circle to optimize the design of DD laminates. Wang et al.⁴¹ proposed a nested p-norm method integrating the Tsai–Hill failure criterion indexes of different elements in different plies into one design response, thus realizing the effective stress control for topology optimization of laminated structures. Tsai's lam⁴² search approach can identify the best DD angles by listing the possible angles with a specified angle interval. However, to the authors' knowledge, there are few researches on the angle design of DD laminates.

In this work, we present a uniform multiple laminates interpolation (UMLI) method, which is inspired by the UMMI scheme, for angle design optimization of DD laminates. This paper is organized as follows. Firstly, the UMLI scheme is proposed in Section 2 for angle optimization of DD laminates. Then, the optimization problem is established in Section 3, together with the involved sensitivity derivation. After that, two computational expensive numerical examples are provided in Section 4, which includes a composite stiffened plate and a composite UAV wing to highlight the effectiveness and significances of the proposed method. Finally, conclusions are given in Section 5.

2. Uniform multiple laminates interpolation (UMLI) method for angle optimization of DD laminates

The evolution process from UMMI to UMLI is introduced in this section. The differences between DD laminates and conventional Quad laminates are analyzed, as well as the reasons why UMLI is suitable for DD laminates. The stiffness matrix of DD laminates is derived. Finally, the selection of alternative angles for DD laminates is described.

2.1 UMMI for multi-material topology optimization

Supposing m_s solid materials and m_e designable elements are considered in multi-material topology optimization, the interpolation of Young's modulus E_i using UMMI scheme²⁰ can be expressed as the weighted summation of all alternative material phases.

$$E_i = \sum_{j=1}^{m_s} w_{ij} E_{ij}^{(j)} \quad (i = 1, \dots, m_e) \quad (1)$$

The weighting function w_{ij} associated with the j th material phase in i th element should satisfy:

$$0 \leq w_{ij} \leq 1 \quad (2)$$

$$\sum_{j=1}^m w_{ij} \leq 1 \quad (3)$$

The relationship between design variables x_{ij} and weighting function w_{ij} in UMMI is as follows:

$$w_{ij} = x_{ij}^p \prod_{\substack{\xi=1 \\ \xi \neq j}}^{m_s} (1 - x_{i\xi}) \quad (4)$$

Where p is the penalty factor on the intermediate weightings with a common value of 3-6 in order to drive all the design variables to be either 0 or 1.

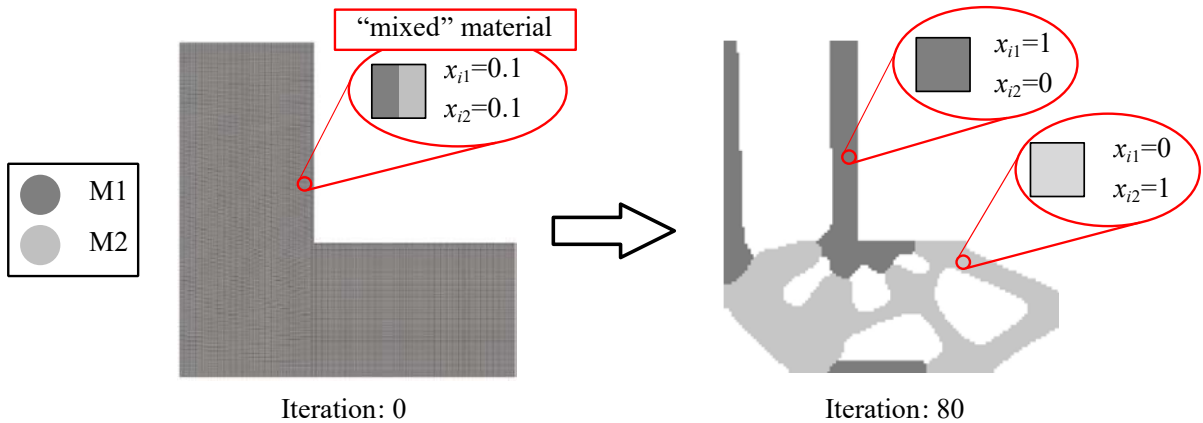


Fig. 1 The topology optimization problem with two alternative materials⁴³

In the optimization process, each material phase has the uniform weighting function and each individual element encompasses m_s design variables. As shown in the Fig. 1, take a

topology optimization problem of two materials⁴³ (M1 and M2) as example. The initial value of the design variables is taken as 0.1 and all elements consist of “mixed” materials. The optimized structure after 80 iterations has a configuration consisting of both M1 ($x_{i1}=1, x_{i2}=0$) or M2 ($x_{i1}=0, x_{i2}=1$).

2.2 UMMI for discrete angle optimization

UMMI scheme can be used in the discrete angle optimization as well. Supposing m_v alternative angles, m_e designable elements and m_p plies are considered, and the constitutive matrix C_{ik} of i th element, k th ply can be expressed as:

$$C_{ik} = \sum_{j=1}^{m_v} w_{ijk} C_{ik}^{(j)} \quad (i = 1, \dots, m_e; k = 1, \dots, m_p) \quad (5)$$

The relationship between design variables x_{ijk} and weighting function w_{ijk} is as follows:

$$w_{ijk} = \prod_{\substack{\xi=1 \\ \xi \neq j}}^{m_v} (1 - x_{i\xi k}) \quad (6)$$

Taking the widely studied benchmark test²⁶ as example, each alternative angle corresponds to a virtual material. As shown in Fig.2, all elements in all plies consist of “mixed” virtual material in the initial iteration and the optimization process leads to a converged solution with discrete optimal angles in all designable patches. This method is suitable for the calculation of single-layer structures. When applying the UMMI scheme to deal with multi-layer structures, it is usually necessary to calculate ply by ply, for all elements in all plies. Each individual element encompasses $m_v \times m_l$ design variables. In addition, laminates’ design constraints for the stacking direction need to be considered in this method, such as symmetry constraint, continuity constraint, and minimum percentage constraint, which increase the difficulty of design²⁹.

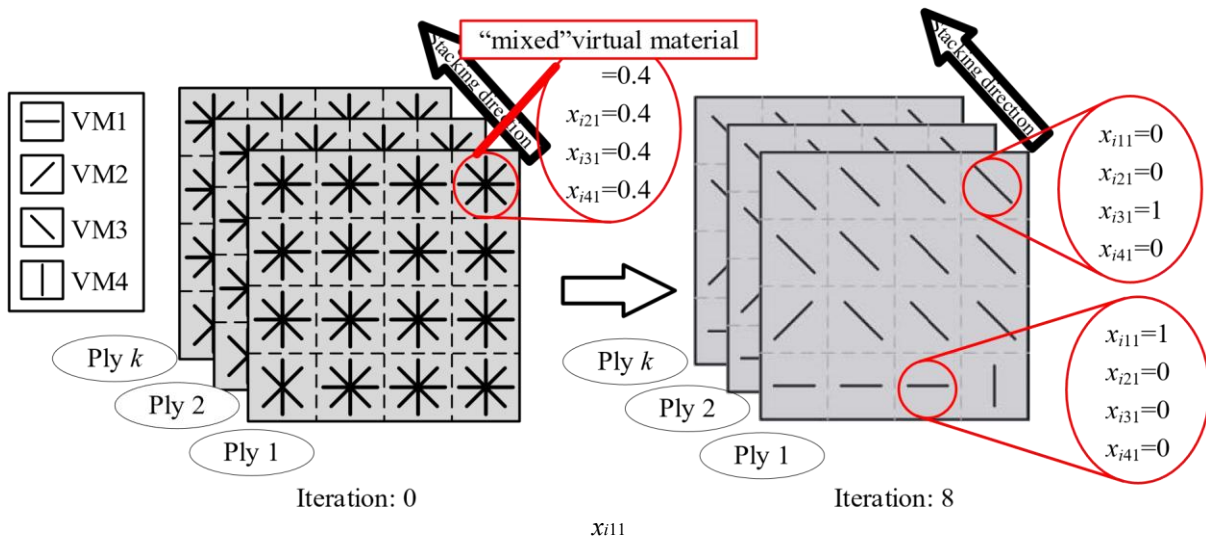


Fig. 2 The application of UMMI to the angle optimization of composite materials

2.3 UMLI for DD-laminates design

DD laminates are multi-layer structures as shown in Fig. 3, such as $[+\Phi/-\Psi/-\Phi/+ \Psi]_{NT}$, where N represents the number of repetitions of the sub-ply and T denotes the total number of plies. This means that once the stacking sequence of the sub-ply and total thickness of the DD laminate are determined, the stacking sequence of the DD laminate is also determined. Optimizing DD laminates using UMMI scheme cannot describe the certainty of the stacking direction of DD laminates. In addition, DD laminates naturally meet most existing design constraints because the stacking direction is formed by repeated sub-ply. So, the optimal design of DD laminates is different from optimizing the fiber angle selection in single-layer laminates or the stacking sequence in multi-layer structures.

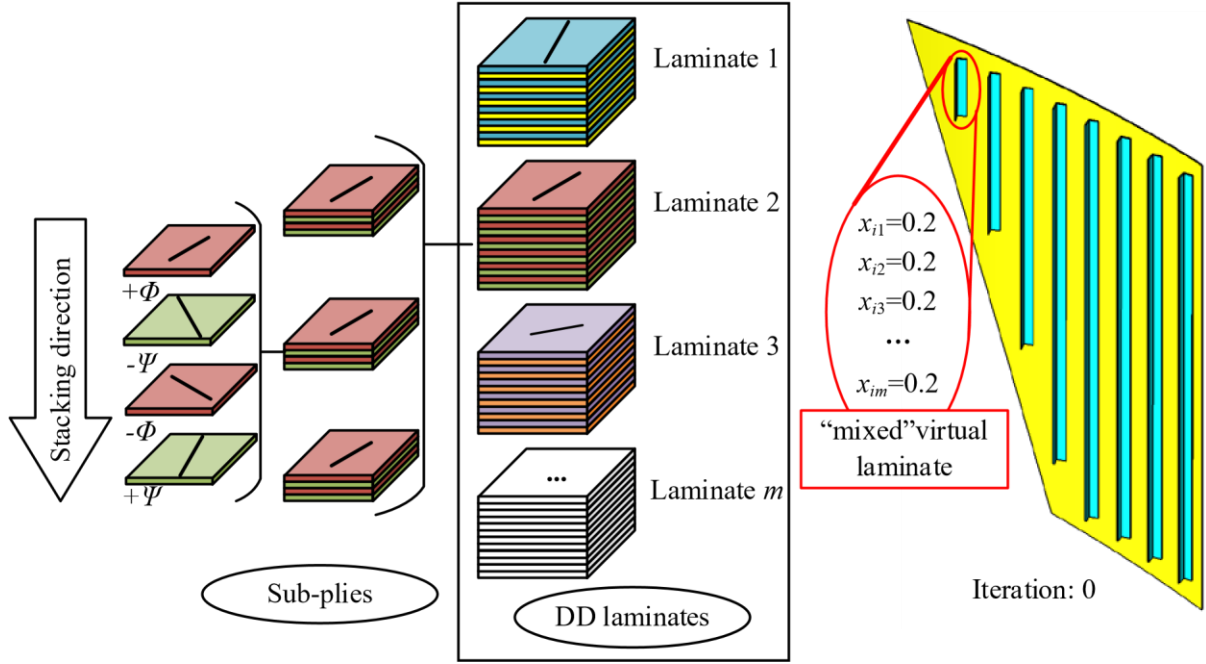


Fig. 3 The application of UMLI to the DD laminates

Therefore, in order to describe the fixed stacking sequence of the plies in DD laminates, we consider the combination of many plies as a whole, rather than as many separate plies. The uniform multiple laminates interpolation (UMLI) scheme inspired by UMMI, which interpolates the stiffness matrix of the laminate is proposed. As shown in Fig. 3, if each area has m_L alternative DD laminates, the $\mathbf{A} \mathbf{B} \mathbf{D}$ matrix of the i th element is represented as a virtual laminate formed by the weighted sum of alternating angle combinations.

$$\begin{aligned} \mathbf{A} \mathbf{B} \mathbf{D} &= \sum_{j=1}^{m_L} w_{ij} \mathbf{A} \mathbf{B} \mathbf{D}_{(j)} \\ \mathbf{B} \mathbf{D} &= \sum_{j=1}^{m_L} w_{ij} \mathbf{B} \mathbf{D}_{(j)} \end{aligned} \quad (7)$$

Herein \mathbf{A} is the tensile stiffness matrix of the laminates, \mathbf{B} is the coupling stiffness matrix, and \mathbf{D} is the bending stiffness matrix. The relationship between design variables x_{ij} and

weighting function w_{ij} in UMMI is as follows, and each individual element encompasses m_L design variables.

$$w_{ij} = \prod_{\substack{\xi=1 \\ \xi \neq j}}^{m_L} \left(1 - \frac{p}{i_\xi}\right) x_{ij} \quad x \quad (8)$$

To have a clear idea, the number of design variables for each individual element needed for UMLI and UMMI schemes is shown in Fig. 4. When the angle increment Δ is 7.5 degrees, the design variables of the each individual element of UMLI are always 91 (the number of alternative laminates). The design variables of the each individual element of UMMI increase with the number of plies, and are 720 at 30 plies.

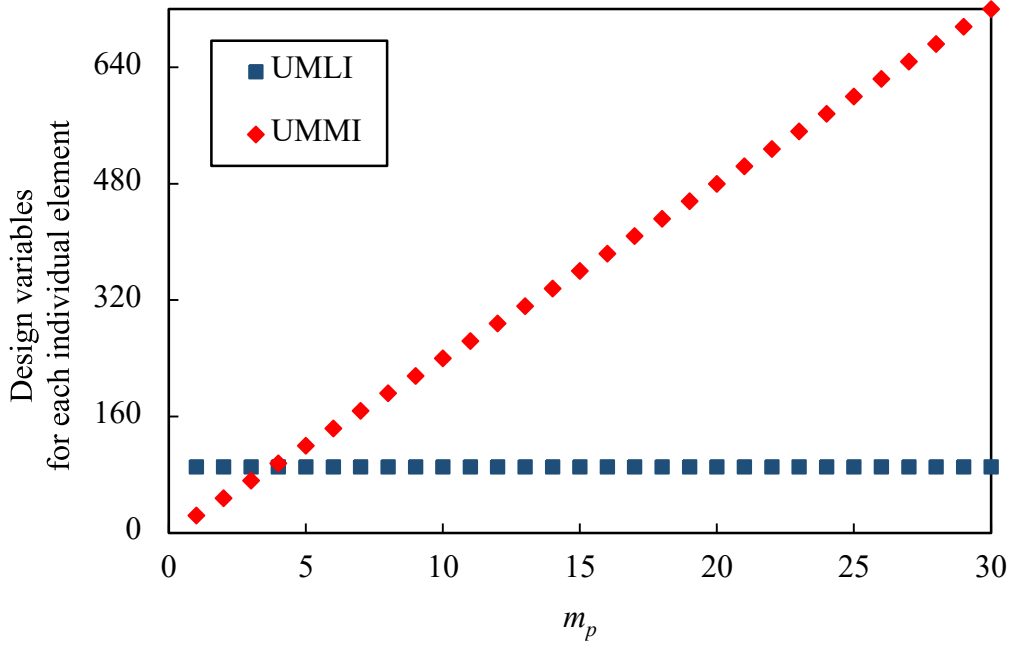


Fig. 4 Comparison of the number of design variables for each individual element related to UMLI and UMMI.

The derivation of the $A B D$ matrix for DD laminates in Equation(7) is presented below. Based on the classical laminate theory, the relationship between internal moment and strain can be expressed as:

$$\begin{aligned} \begin{bmatrix} P_x \\ P_y \\ P_{xy} \end{bmatrix}_{m_p} &= \sum_{k=1}^{m_p} \int_{z^{k-1}}^{z^k} \begin{bmatrix} Q_{xx} \\ Q_{xy} \\ Q_{yy} \end{bmatrix} dz \epsilon_0 + \sum_{k=1}^{m_p} \int_{z^{k-1}}^{z^k} \begin{bmatrix} Q_{xx} \\ Q_{xy} \\ Q_{yy} \end{bmatrix} dz z \kappa = A \epsilon_0 + B \kappa \\ \begin{bmatrix} M_x \\ M_y \\ M_{xy} \end{bmatrix}_{m_p} &= \sum_{k=1}^{m_p} \int_{z^{k-1}}^{z^k} \begin{bmatrix} Q_{xx} \\ Q_{xy} \\ Q_{yy} \end{bmatrix} dz z \epsilon_0 + \sum_{k=1}^{m_p} \int_{z^{k-1}}^{z^k} \begin{bmatrix} Q_{xx} \\ Q_{xy} \\ Q_{yy} \end{bmatrix} dz z^2 d \kappa = B \epsilon_0 + D \kappa \end{aligned} \quad (9)$$

$$\begin{bmatrix} M_{xy} \\ M_{xx} \end{bmatrix} = \sum_{k=1}^n \begin{bmatrix} Q_k (z_k - z_{k-1}) \\ Q_k (z_k^2 - z_{k-1}^2) \end{bmatrix} \quad (10)$$

Herein \mathbf{P} and \mathbf{M} are vectors of the in-plane forces and moments per unit width. m_p is the total number of plies of the laminates. z_k, z_{k-1} is the coordinates of the upper and lower surfaces of ply k . $\boldsymbol{\varepsilon}^0$ is the middle plane strain matrix, $\boldsymbol{\kappa}$ is the middle plane curvature matrix. The above formulas can be combined and abbreviated as:

$$\begin{bmatrix} \mathbf{P} \\ \mathbf{M} \end{bmatrix} = \begin{bmatrix} \mathbf{A} & \mathbf{B} \\ \mathbf{B}^T & \mathbf{D} \end{bmatrix} \begin{bmatrix} \boldsymbol{\varepsilon}^0 \\ \boldsymbol{\kappa} \end{bmatrix} \quad (11)$$

The calculated $\mathbf{A} \mathbf{B} \mathbf{D}$ matrix can be expressed as:

$$\begin{aligned} \mathbf{A} &= \sum_{k=1}^n \mathbf{Q}_k (z_k - z_{k-1}) \\ \mathbf{B} &= \sum_{k=1}^n \mathbf{Q}_k (z_k^2 - z_{k-1}^2) \\ \mathbf{D} &= \sum_{k=1}^n \mathbf{Q}_k (z_k^3 - z_{k-1}^3) \end{aligned} \quad (12)$$

As DD laminates are composed of two angles in a certain stacking sequence to form fourply sub-ply, and then the repeatedly formed laminates are shown in Fig. 5, so the stiffness matrix $\mathbf{A} \mathbf{B} \mathbf{D}$ of DD laminates can be simplified, and the results are as follows:

$$\begin{aligned} \mathbf{A} &= Nt (\mathbf{Q}_1 + \mathbf{Q}_2 + \mathbf{Q}_3 + \mathbf{Q}_4) \\ \mathbf{B} &= \frac{3Nt^2}{2} (\mathbf{Q}_1 - \mathbf{Q}_4) + \frac{Nt^2}{2} (\mathbf{Q}_2 - \mathbf{Q}_3) \\ \mathbf{D} &= \frac{4Nt^3}{3} (\mathbf{Q}_1 + \mathbf{Q}_4) + \frac{4Nt^3}{3} (\mathbf{Q}_2 + \mathbf{Q}_3) \end{aligned} \quad (13)$$

Herein, N is the number of sub-ply, $N = m_p/4$. t is the thickness of the ply. $\mathbf{Q}_1, \mathbf{Q}_2, \mathbf{Q}_3, \mathbf{Q}_4$ are the unidirectional plate off-axis stiffness matrices that form the sub-ply of 4 plies, and if

the stacking sequence of the sub-ply is $[\pm\Phi/-\Psi/-\Phi/+ \Psi]$, then $\mathbf{Q}_1 = \mathbf{Q}_2 = \mathbf{Q}_3 = \mathbf{Q}_4 = \mathbf{Q}$, $\mathbf{Q}_1 = \mathbf{Q}_2 = \mathbf{Q}_3 = \mathbf{Q}_4 = \mathbf{Q}$, $\mathbf{Q}_1 = \mathbf{Q}_2 = \mathbf{Q}_3 = \mathbf{Q}_4 = \mathbf{Q}$, $\mathbf{Q}_1 = \mathbf{Q}_2 = \mathbf{Q}_3 = \mathbf{Q}_4 = \mathbf{Q}$.

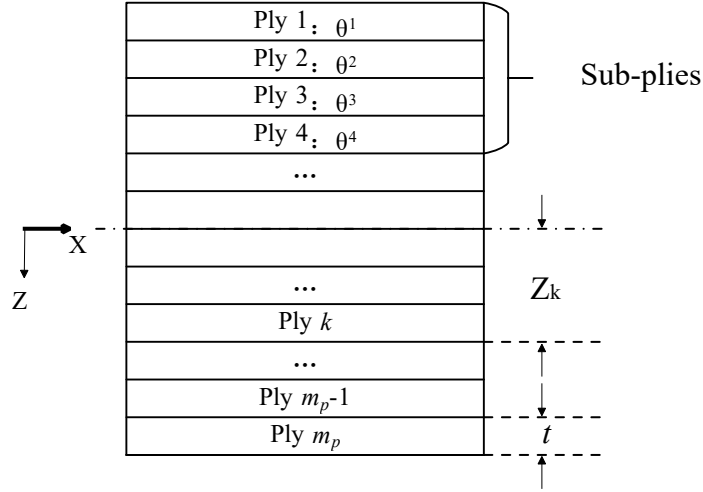


Fig. 5 DD laminates diagram.

2.4 Selection of alternative angles for DD laminates

The alternative angle range for conventional laminates is -90 to 90 degrees. The relationship between the number of alternative angles m and the angle increment is shown in Equation(13). When the angle increment Δ is 7.5 degrees, there are 24 possibilities $[0, 7.5, 15, \dots, 82.5, 90, -82.5, \dots, -15, -7.5]$. The usual angle increment is taken as 45 degrees, and the angle selection for laminate is $[0, 45, 90, -45]$, which is called Quad.

$$m_v = \frac{180^\circ}{\Delta} \quad (13)$$

While the value range of the alternative angle combinations $[\phi/\psi]$ for DD laminates is 0 to 90 degrees. The relationship between the number of alternative angles m_L and the angle increment is shown in Equation(14). If the angle increment is 7.5 degrees, then there are 13 choices for each of ϕ and ψ . After permutation and combination, the number of possible angle combinations for DD laminates is 91 as shown in Fig. 12.

$$m_L = \frac{90}{\Delta} \times \frac{90}{\Delta} + 2 \times \frac{90}{\Delta} \times \frac{90}{\Delta} + 1 \times \frac{90}{\Delta} \times \frac{90}{\Delta} \quad (14)$$

The so-called single-double (SD) laminates should be highlight. The left side is DD laminates, and the right side is SD laminates as shown in Fig. 6. SD means $\phi=\psi$ and is a better choice in some applications, because compared to DD, SD has more fibers which can achieve a smaller angle with the principal stress. Among SD, there is special case. Plus or minus 0 degrees results is the same angle, as well as plus or minus 90 degrees. If $\phi=\psi$ is equal to 0 or 90 degrees, it means that each ply of the laminates has the same angle. While this is typically not allowed in engineering due to manufacturability constraints, the mechanical properties of this stacking

sequence are strongest in the 0 or 90 degree orientation. In the subsequent example, we will analyze the impact of excluding laminates with the same angle plying and laminates with SD stacking sequences from the alternative angle combination on the optimization results. $+\Psi = 60^\circ$

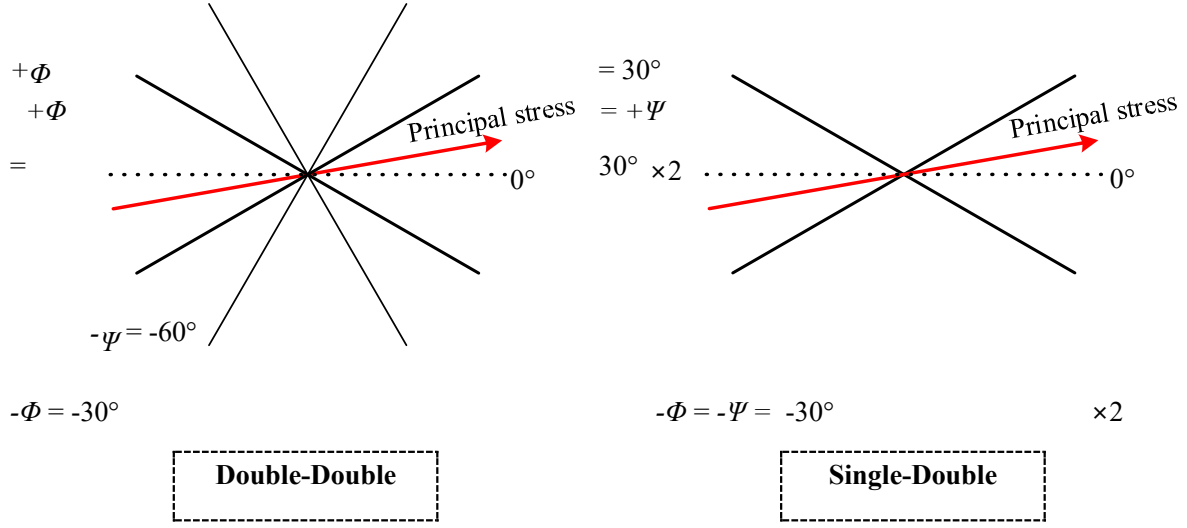


Fig. 6 Comparison of fiber layout of DD laminates and SD laminates

3. Optimization process using UMLI method

In this section, an optimization problem aiming at minimum compliance is described, and the sensitivity of the optimization problem is derived, and finally the optimization process is described.

3.1 Optimization formulation

Considering the minimum compliance of composite laminates, the angle combinations of DD laminates is optimized. Optimization problems can be described as: find : $\{x_{ij}\}$ ($i = 1, \dots, m_e; j = 1, \dots, m_L$)

$$\text{minimize: } C = \mathbf{F} \mathbf{u}^T \quad (15)$$

$$\text{subject to : } \mathbf{F} = \mathbf{K} \mathbf{u}$$

Herein x_{ij} is the design variable. m_e is the number of elements and m_L is the number of angle combinations for DD laminates. C is the overall compliance. \mathbf{K} is the element stiffness matrix. \mathbf{F} and \mathbf{u} are the external force vector and the displacement vector, respectively.

3.2 Sensitivity analysis

The sensitivity of the overall compliance can be generally expressed as:

$$\frac{\partial C}{\partial x_{ij}} = 2 \mathbf{u}^T \frac{\partial \mathbf{F}}{\partial x_{ij}} - \mathbf{u}^T \frac{\partial \mathbf{K} \mathbf{u}}{\partial x_{ij}} \quad (16)$$

For fixed loads, then we have $\frac{\partial \mathbf{F}}{\partial x_{ik}} \equiv 0$. Thus, the sensitivity can be simplified as $\frac{\partial C}{\partial x_{ik}}$

$$\frac{\partial x_{Cij}}{\partial} = -\underline{u}_T \frac{\partial}{\partial} x_{\underline{K}ij} \underline{u} \underline{u} = -\frac{\partial}{\partial} x_{ij} \underline{u}_i \underline{u}_j \quad (17)$$

Here, the stiffness matrix of element i is defined as:

$$\{\kappa\} = [B \ u_b] \{ \begin{smallmatrix} b \end{smallmatrix} \} \quad (19)$$

$$\{\varepsilon^0\} = \mathbf{B}_p \{u_p\} \quad (20)$$

According to the derivation of Equation(18), $\frac{\partial \mathbf{K}_i}{\partial \mathbf{K}_i}$ in Equation (17) can be expressed as:

$$\partial \underline{\mathbf{K}}_{ijl} = \int \int \left(\frac{\partial}{\partial x} \frac{\partial w_{xijin}}{\partial y} \right) \mathbf{B}_{bp}^T \mathbf{A}_m \mathbf{B}_n dx dy \quad (21)$$

Mathematically, the following relation can easily be derived:

$$(22) \quad \partial x_{ij} \quad n=1$$

$$\partial x_{ij} \quad \square \quad b \quad \square_i \quad \square \square_i \quad \square \quad b \quad \square_i \quad n=1 \quad \partial x_{ij}$$

$$\prod_{\substack{\xi=1 \\ \xi \neq n}}^{-1} i_{\xi}^{\frac{p}{2}} \prod_{j=n+1}^m (1 - x_j^{\frac{p}{2}})$$

$$\partial x_{ij} \stackrel{\xi=1}{\neq} i_{\xi}^{\xi} \square - p x_{ij}^{p-1} x_{in}^p \prod (1 - x^p) \quad \text{if } j \neq n$$

$$\begin{matrix} \square \\ \square \square \end{matrix} \quad \begin{matrix} \xi \\ \xi \neq j \end{matrix} \quad n$$

3.3 Optimization process

To begin the optimization process, the alternative angle combinations and stacking sequences for DD laminates must be selected according to the specific technological requirements. Next, the stiffness matrix is calculated for each angle combination, and the interpolated stiffness matrix is obtained through the UMLI scheme. Subsequently, the sensitivity is computed, the design variables are updated, and the response value is calculated by finite element analysis (FEA). The angle design of DD laminates is finalized once the convergence criterion is reached. In this work, the optimization is considered to have converged when the weights of each angle combination converge to 0 or 1. The calculations are stopped once the convergence condition is achieved. The specific flowchart is shown in Fig. 7.

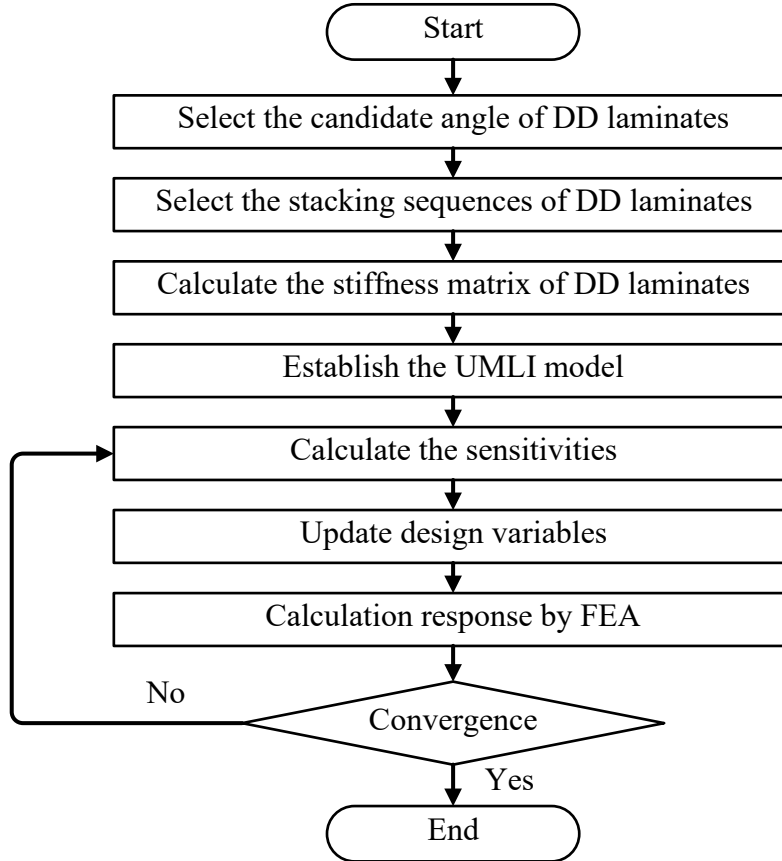


Fig. 7 Optimization process flow chart.

4. Numerical Examples

Two numerical examples with engineering background are used here to validate the effectiveness of the proposed UMLI. The two examples are DD layup angle design of composites stiffened panel and composites UAV wing. The compliance is calculated using commercial finite element software ANSYS, and the optimization algorithm is GCMMA.

4.1 Composite stiffened panel

Composite stiffened panels are frequently employed in the manufacture of wings and fuselages. The cross-section of the stiffener commonly assumes an "L" shape, "T" shape, "Ω" shape, and so on. In this example, the composite stiffened plate comprises one 40-ply curved plate and eight 40-ply L-shaped stiffeners of varying lengths, as illustrated in Fig. 8. The common forming processes for composite stiffened panels can be used to connect different areas: co-curing, co-bonding, or secondary bonding. The stiffened panels are subjected to a pressure of 5000Pa and a shear force of 3000N.

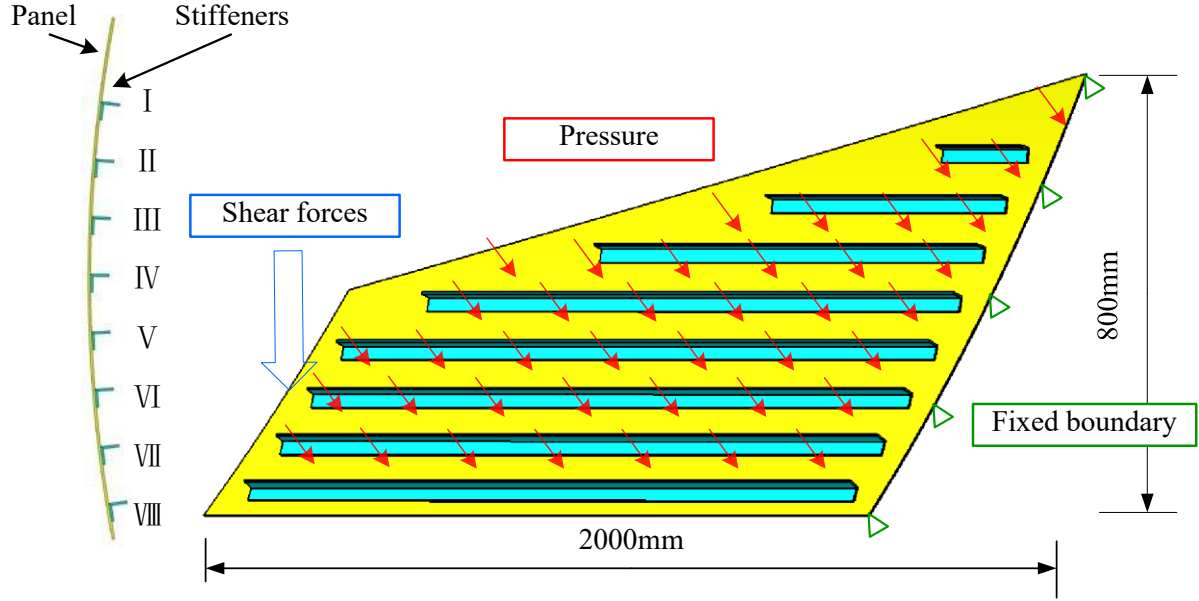


Fig. 8 Composite stiffened panel with 8 L-shaped stiffeners.

Given the actual manufacturing circumstances, the composite stiffened panels are categorized into nine areas: panel and stiffeners I to VIII, with each area selecting a DD laminate angle combination. The objective is to optimize for minimum compliance. This example utilizes DD laminates with the stacking sequence $[\Phi/\Psi/-\Phi/+ \Psi]_{10}$. First, an angle increment of 15 degrees is adopted. Then according to Equation(14) based 28 angle combinations, as given in Table 1. The UMLI scheme is employed to select the appropriate $[\Phi/\Psi]$ from the 28 angle combinations to minimize the compliance of the structure.

Table 1 $[\Phi/\Psi]$ Angle combinations with an angle increment of 15°

Num	$[\Phi/\Psi]$	Num	$[\Phi/\Psi]$	Num	$[\Phi/\Psi]$	Num	$[\Phi/\Psi]$
1	$[0^\circ, 0^\circ]$	8	$[15^\circ, 15^\circ]$	15	$[30^\circ, 45^\circ]$	22	$[45^\circ, 90^\circ]$
2	$[0^\circ, 15^\circ]$	9	$[15^\circ, 30^\circ]$	16	$[30^\circ, 60^\circ]$	23	$[60^\circ, 60^\circ]$
3	$[0^\circ, 30^\circ]$	10	$[15^\circ, 45^\circ]$	17	$[30^\circ, 75^\circ]$	24	$[60^\circ, 75^\circ]$
4	$[0^\circ, 45^\circ]$	11	$[15^\circ, 60^\circ]$	18	$[30^\circ, 90^\circ]$	25	$[60^\circ, 90^\circ]$
5	$[0^\circ, 60^\circ]$	12	$[15^\circ, 75^\circ]$	19	$[45^\circ, 45^\circ]$	26	$[75^\circ, 75^\circ]$
6	$[0^\circ, 75^\circ]$	13	$[15^\circ, 90^\circ]$	20	$[45^\circ, 60^\circ]$	27	$[75^\circ, 90^\circ]$

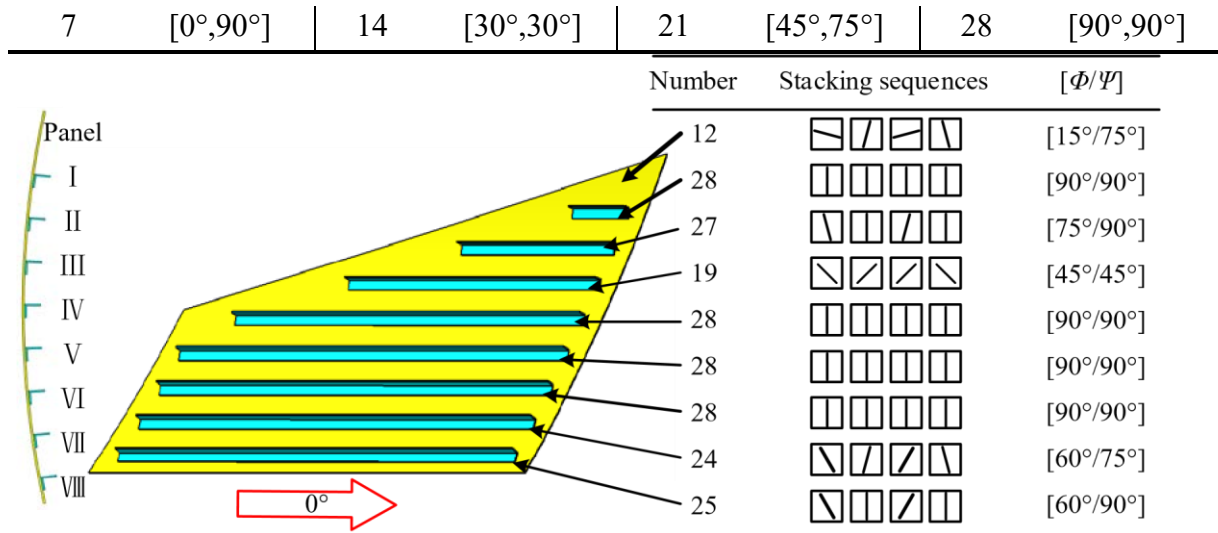


Fig. 9 Optimization results of angle selection for the stiffened panel

After 41 steps of calculation, the compliance convergence is 2380J stably. The selections of angle combinations are shown in Fig. 9. The convergence curve is shown in Fig. 10. Due to the shear force added to the main load of the stiffened panels for this example, the orientation of the fibers is as expected. It is proved that it is feasible to interpolate $A B D$ matrix of DD laminates by UMLI scheme so as to realize the angle optimization design of DD laminates.

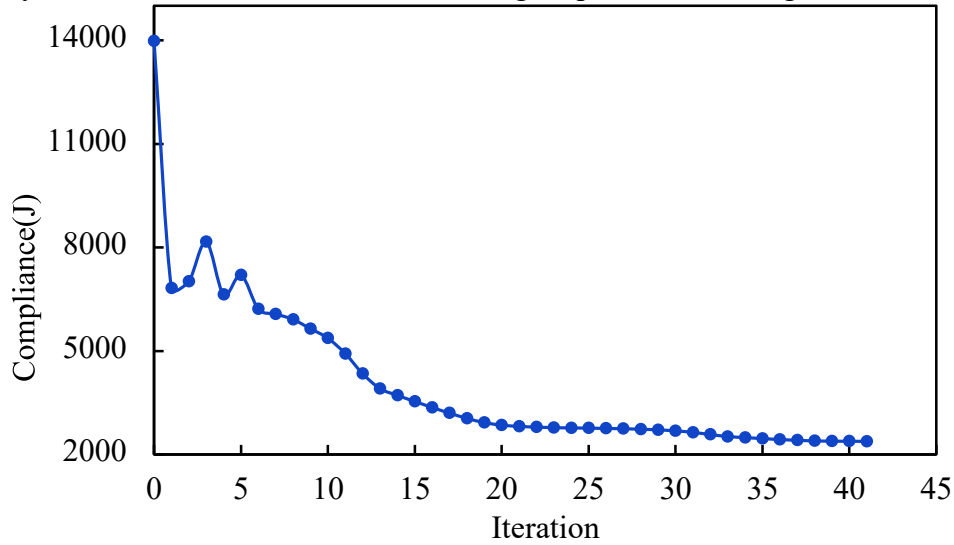


Fig. 10 The convergence curve

The change curve of design variables x_{ij} of angle combinations in the panel is shown in Fig. 11. Step 0: The design variable of all combinations of angles is 0.2. Step 41: The design variable of angle combination $[15, 75]$ converges to 1. According to Equation(8). When the design variables are 0 or 1, the weights are equal to the design variables. It means that the weight of angle combination $[15, 75]$ converges to 1, and the remaining angle combinations converge to 0 in step 41. The panel eventually converges to angle combination $[15, 75]$, so the stacking sequence of the panel is $[15, -75, -15, 75]_{10}$.

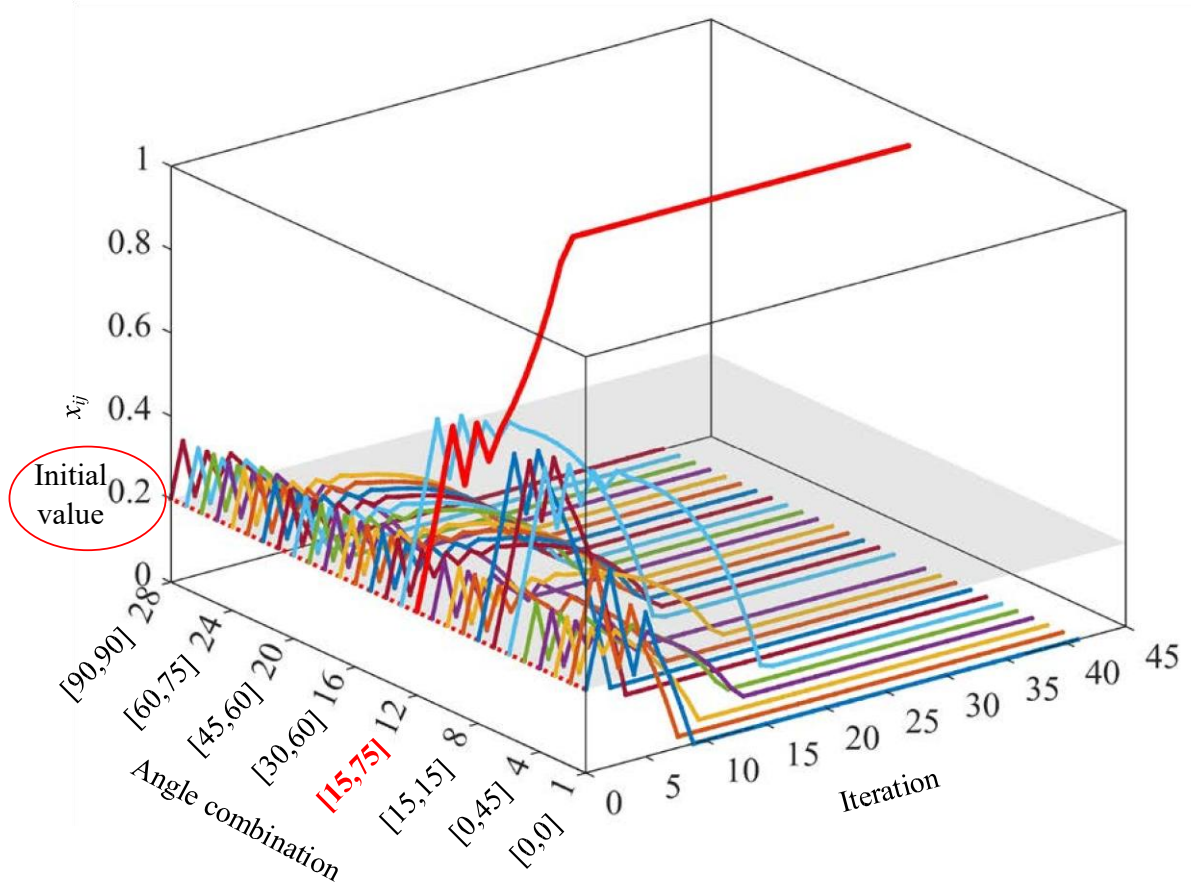


Fig. 11 The design variable convergence curves of angle combination

In order to compare the effects of SD laminates and laminates with the same angle on the optimization results and compliance, an angle increment of 7.5 degrees was selected, consistent with the angle increment in Tsai's paper³⁶. Through the calculation of formula 15, there are 91 angle combinations, as shown in Fig. 12. The horizontal axis represents the value of Φ , while the vertical axis represents the value of Ψ . The squares indicate the angle combination numbers. The red squares represent laminates with the same angle, the blue squares represent SD laminates, and the green squares represent DD laminates. We used 91, 89 (excluding laminates with the same angle), and 78 (excluding SD laminates) as alternative angle combinations, with the goal of optimizing for minimum compliance. For the three examples, the initial value is set to 0.4 and the step size is 0.2. The angle combination selection for the obtained panel and stiffeners is presented in the following Table 2. The convergence curve is illustrated in Fig. 13.

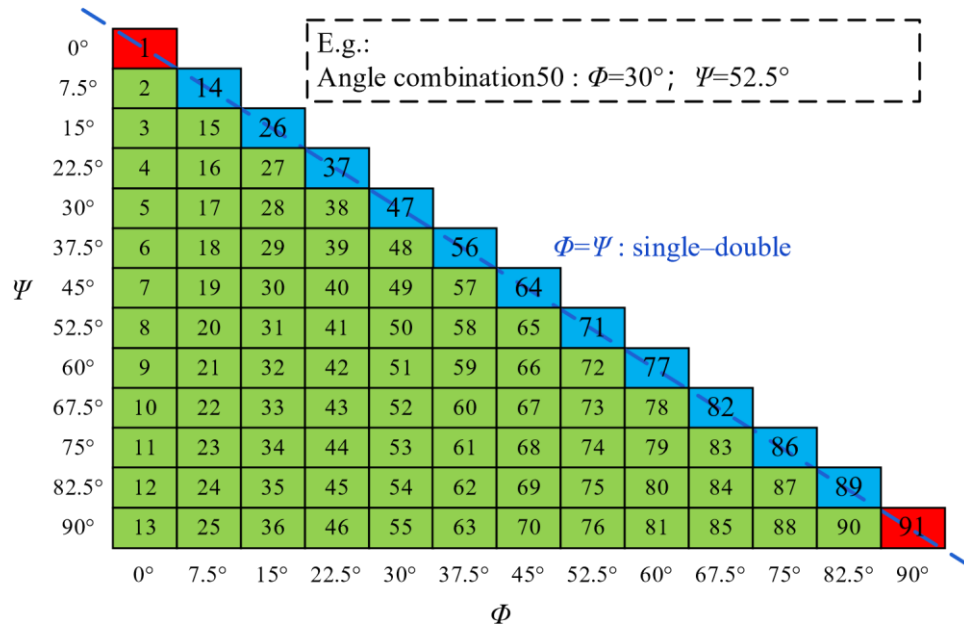
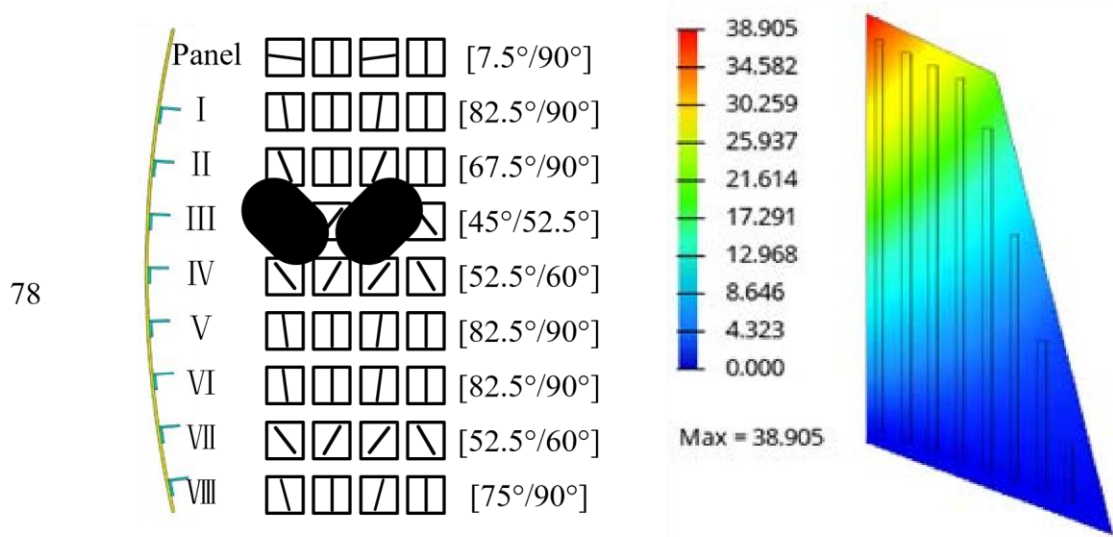
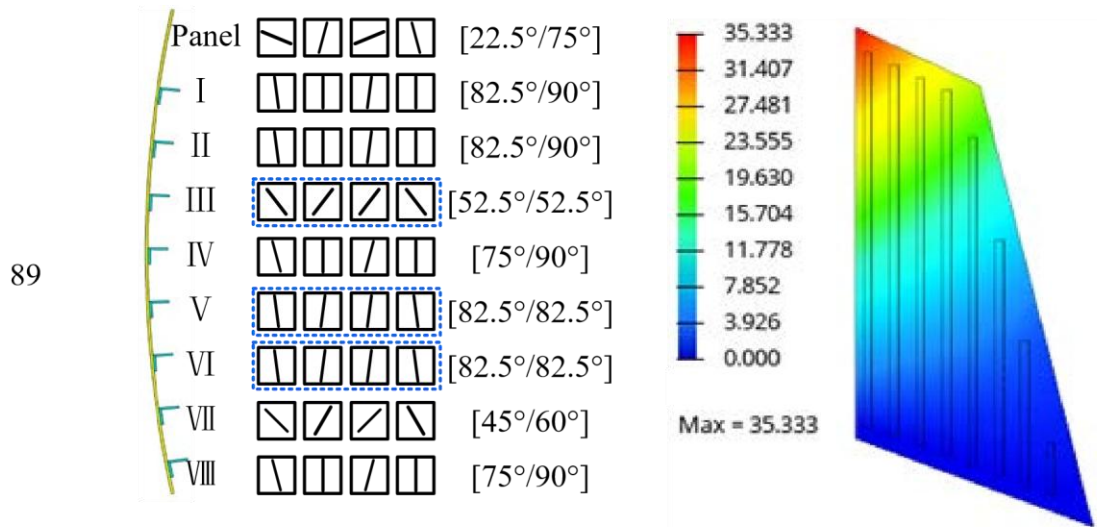


Fig. 12 [Φ/Ψ] Angle combinations with an angle increment of 7.5.

Table 2 Optimization results and finite element analysis results of composite stiffened panels.

Angle				
combinatio	Optimization results		Displacement nephogram	
n				
91	Panel		[30°/75°]	
	I		[90°/90°]	
	II		[75°/90°]	
	III		[60°/60°]	
	IV		[82.5°/82.5°]	
	V		[90°/90°]	
	VI		[90°/90°]	
	VII		[52.5°/60°]	
	VIII		[67.5°/90°]	



The compliance converges to 2260J from 91 alternative angle combinations. The compliance converges to 2290J from 89 alternative angle combinations. The compliance converges to 2630J from 78 alternative angle combinations.

The results of the 91 alternative angles combinations and the 89 alternative angles combinations are better because this situation provides a stronger choice along the 0 degree orientation and 90 degree orientation. The difference between the results including SD and those excluding SD is about 14.8% in this example. Finite element analysis was conducted on the three optimized results, as shown in Table 2. It was found that the maximum displacements were 35.63mm, 35.33mm, and 38.91mm, which followed the same trend as the compliance results. When dealing with practical engineering problems, it is necessary to choose the appropriate alternative angle combinations according to the specific process requirements.

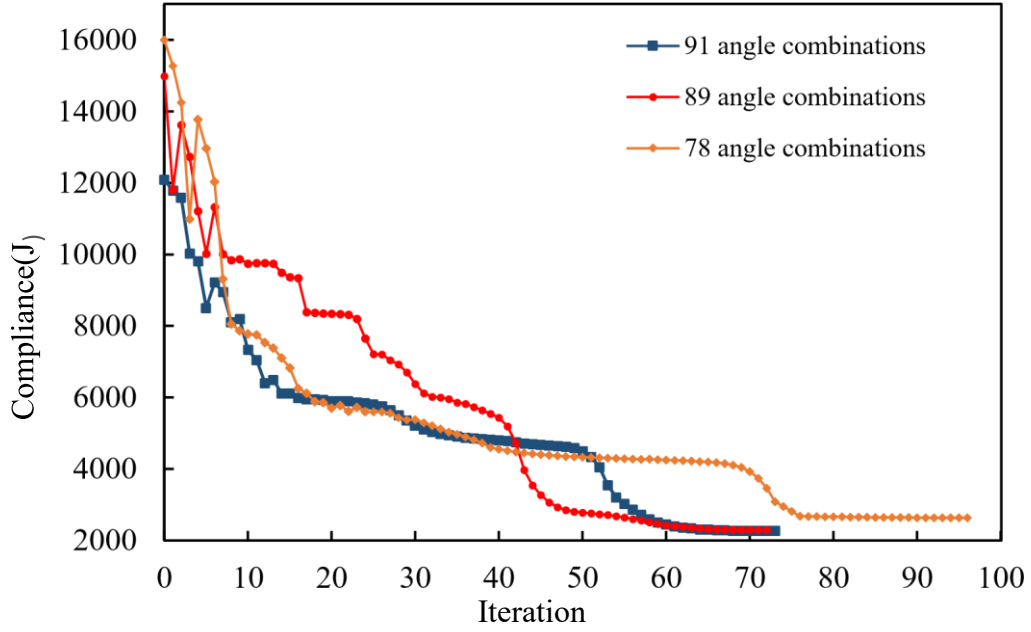


Fig. 13 Convergence curve of compliance.

4.2 Composite UAV wings

Due to its low cost, simple structure, and other advantages, the UAVs are widely used in military, meteorological, surveying, and other fields. The introduction of composite materials, which have high specific modulus and stiffness, can enable UAVs to have better performance, greater load capacity, and longer range. In this example, the UAV has a wingspan of 2m, and we calculate half of the wing. The wing is a two-spar wing, consisting of an upper skin, a lower skin, a front spar, a rear spar, and four wing ribs distributed along the span direction, as shown in Fig. 14. All areas are made of 20 plies of 0.1 thick composite materials. The wing bears the upward lift acting on the skin surface, which is applied in the form of pressure, referred to as the lift condition in this paper; Due to the deflection of the wing control surface or gust load, the wing bears the torsional load, which is applied in the form of concentrated force, referred to as the concentrated force condition.

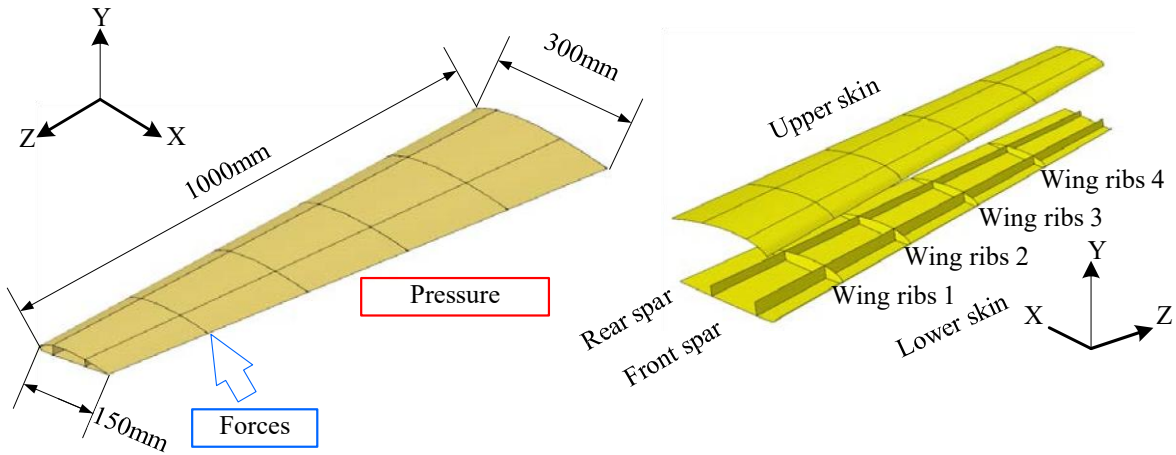

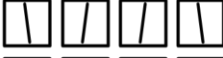
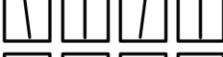




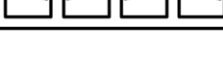


Fig. 14 Composite UAV wings

In this example, an angle increment of 7.5 degrees was selected. The alternative angle combinations are shown in Fig. 12. Considering the constraint of processability, the angle combinations [0/0] and [90/90] were removed. The remaining 89 alternative angle combinations were selected. The optimization results considering lift condition and concentrated force condition were calculated and shown in Table 3. The initial value was set to 0.4 and the step size was set to 0.12. The convergence curve is shown in blue in Fig. 15. After 74 steps of calculation, the compliance converged to 268.8J stably. To verify the correctness of the results, the lift condition, concentrated force condition, and coupled condition were verified for the DD-piled wing.

Table 3 Optimization results of DD-piled wing with UMLI

Area	Stacking sequences	$[\Phi/\Psi]$
Upper skin		$[75^\circ/75^\circ]$
Lower skin		$[82.5^\circ/82.5^\circ]$
Front spar		$[82.5^\circ/90^\circ]$
Rear spar		$[7.5^\circ/15^\circ]$
Wing ribs 1		$[7.5^\circ/37.5^\circ]$
Wing ribs 2		$[0^\circ/7.5^\circ]$
Wing ribs 3		$[0^\circ/7.5^\circ]$
Wing ribs 4		$[15^\circ/15^\circ]$

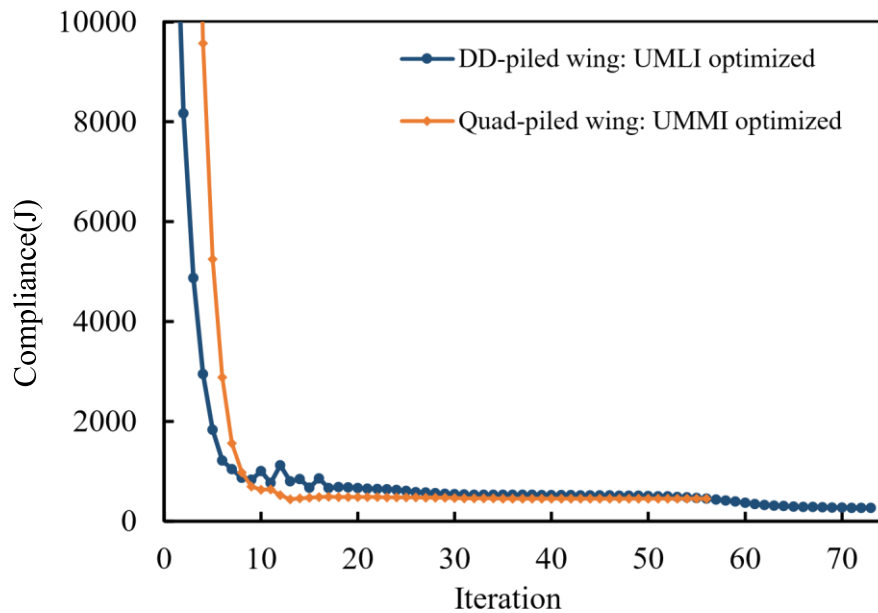


Fig. 15 The convergence curve

For comparison, the Quad-piled wing was also calculated and the UMMI method is adopted to optimize the angle. The results of angle selection are shown in Table 4. Upon examination, it

is evident that the UMMI optimization results exhibit numerous violations of design constraints, potentially posing significant challenges to manufacturability and giving rise to issues such as warping, delamination, and other defects in the formed composite parts. The convergence curve is shown in Fig. 15. The orange curve shows that the compliance converged to 454.8J, which is slightly greater than that of the DD-piled wing.

Table 4 Optimization results of Quad-piled wing with UMMI

In	Ply number	Upper skin	Lower skin	Front spar	Rear spar	Wing rib 1	Wing rib 2	Wing rib 3	Wing rib 4
	1	90°	90°	90°	0°	0°	90°	90°	-45°
	2	90°	90°	90°	0°	0°	0°	90°	-45°
	3	90°	-45°	90°	0°	0°	0°	90°	-45°
	4	90°	-45°	90°	0°	45°	0°	0°	-45°
	5	90°	-45°	90°	0°	45°	0°	0°	-45°
	6	90°	-45°	90°	0°	45°	0°	0°	-45°
	7	90°	-45°	90°	0°	45°	0°	0°	-45°
	8	90°	-45°	90°	0°	45°	0°	0°	-45°
	9	90°	-45°	90°	0°	45°	0°	0°	-45°
	10	90°	-45°	90°	0°	45°	0°	0°	-45°
	11	90°	-45°	90°	0°	45°	0°	0°	0°
	12	45°	0°	90°	0°	0°	0°	0°	0°
	13	45°	0°	90°	0°	0°	0°	45°	0°
	14	45°	-45°	90°	0°	0°	0°	45°	0°
	15	45°	-45°	90°	0°	0°	0°	45°	0°
	16	45°	-45°	90°	0°	0°	-45°	45°	0°
	17	45°	-45°	90°	0°	0°	-45°	45°	-45°
	18	45°	-45°	90°	0°	0°	-45°	45°	-45°
	19	45°	-45°	90°	0°	0°	45°	90°	90°
	20	45°	90°	90°	0°	0°	90°	90°	90°

addition, in order to compare with the optimization results of commercial software, the stacking sequence of the Quad-piled wing was optimized using software-OPTISTRUCT. The initial four angles of the Quad-piled wing are equal in percentage, each accounting for 25%. The optimized stacking sequence is shown in Table 5. Simultaneously, the several commonly used Quad-piled wing is adopted for calculation: Commonly used Quad-piled wing – repeat, with the stacking sequence of [0,45,90,-45]_s; Commonly used Quad-piled wing – symmetry, with the stacking sequence of [0,45,90,-45,0,45,90,-45,0,45]_s.

Table 5 Optimization results of Quad-piled wing with OPTISTRUCT

Ply number	Upper rib 2	Lower rib 3	Front rib 4	Rear spar	Wing spar	Wing rib 1	Wing rib 2	Wing rib 3	Wing rib 4
1	-45°	90°	-45°	-45°	90°	90°	90°	90°	90°
2	-45°	0°	90°	0°	45°	90°	90°	-45°	
3	-45°	0°	90°	0°	45°	90°	90°	-45°	
4	-45°	0°	90°	0°	45°	90°	90°	-45°	

5	-45°	0°	90°	0°	45°	90°	90°	-45°
6	45°	0°	90°	-45°	45°	45°	45°	45°
7	45°	45°	0°	0°	45°	0°	0°	0°
8	90°	45°	0°	45°	0°	0°	0°	-45°
9	90°	-45°	0°	90°	0°	0°	0°	-45°
10	45°	90°	45°	45°	0°	0°	0°	0°
11	45°	-45°	45°	45°	0°	0°	0°	0°
12	45°	-45°	45°	45°	0°	0°	0°	0°
13	90°	-45°	45°	-45°	-45°	-45°	-45°	45°
14	90°	45°	-45°	-45°	-45°	-45°	-45°	45°
15	90°	45°	-45°	-45°	-45°	-45°	-45°	45°
16	0°	45°	-45°	90°	-45°	90°	90°	45°
17	0°	45°	-45°	90°	-45°	90°	90°	45°
18	0°	45°	-45°	90°	-45°	90°	90°	45°
19	0°	90°	0°	90°	90°	45°	45°	90°
20	0°	90°	-45°	-45°	90°	45°	45°	90°

The results of the verification analysis of the DD-piled wing, the optimized Quad-piled wing and two commonly used Quad-piled wings are calculated. The histogram of maximum displacement comparison is shown in Fig. 16.

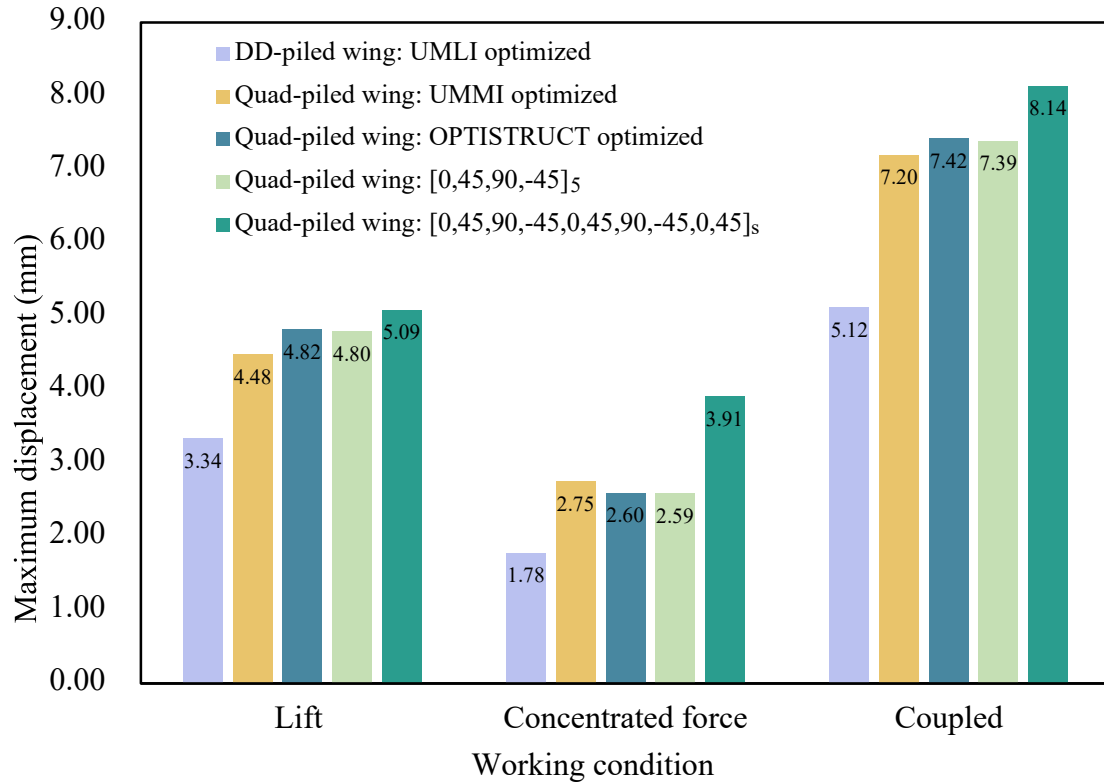


Fig. 16 The maximum displacement comparison

As evident from the figure, In this example, The maximum displacement of Quad-piled wing optimized by UMMI, Quad-piled wing optimized by OPTISTRUC, and Quad-piled wing with repeated layings is very similar, and the displacement of Quad-piled wing with symmetrical layings is slightly larger. In contrast, the DD-piled wing optimized by UMLI

exhibits a reduction of approximately 30% in its maximum displacement, thereby validating the effectiveness of optimizing the DD-piled wing.

5. Conclusion

This paper proposes an optimization design method for DD laminates based on multimaterial topology optimization method. An interpolation method UMLI for multi-layer structures is proposed. The optimization design of DD laminates is completed by interpolating the stiffness matrix of the laminates formed by each angle combination. The main conclusions are as follows:

- (1) UMLI is suitable for the optimization design of multi-layer structures with certainty stacking sequence in the stacking direction, such as DD laminates. This approach allows for the design of multilayer composites with fewer design variables. And the optimization results show that the optimized DD laminates can achieve better performance than Quad laminates.
- (2) The selection of alternative angles has a significant impact on the optimization results, and SD laminates and laminates with the same angle are better choices in some cases. In practical use, it is necessary to choose suitable alternative angles based on engineering process requirements.

In future work, this method can be applied to the angular design of variable stiffness DD laminates. Simultaneously, the performance and processability of DD laminates can be verified through experiments and simulation analysis.

References

- 1 Xu Yingjie, Zhu Jihong, Wu Zhen, Cao Yinfeng, Zhao Yubo, Zhang Weihong. A review on the design of laminated composite structures: constant and variable stiffness design and topology optimization. *Adv Compos Hybrid Mater* 2018;**1**(3):460–77. Doi: 10.1007/s42114018-0032-7.
- 2 Tiwary Akash, Kumar Raman, Chohan Jasgurpreet Singh. A review on characteristics of composite and advanced materials used for aerospace applications. *Mater Today Proc* 2022;**51**:865–70. Doi: 10.1016/j.matpr.2021.06.276.
- 3 Potgieter E., Stander N. The genetic algorithm applied to stiffness maximization of laminated plates: review and comparison. *Struct Optim* 1998;**15**(3–4):221–9. Doi: 10.1007/BF01203535.
- 4 Erdal Ozgur, Sonmez Fazil O. Optimum design of composite laminates for maximum buckling load capacity using simulated annealing. *Compos Struct* 2005;**71**(1):45–52. Doi: 10.1016/j.compstruct.2004.09.008.
- 5 Hasançebi Oğuzhan, Çarbaş Serdar, Saka Mehmet Polat. Improving the performance of simulated annealing in structural optimization. *Struct Multidiscip Optim* 2010;**41**(2):189–203. Doi: 10.1007/s00158-009-0418-9.
- 6 Suresh S., Sujit P.B., Rao A.K. Particle swarm optimization approach for multi-objective composite box-beam design. *Compos Struct* 2007;**81**(4):598–605. Doi: 10.1016/j.compstruct.2006.10.008.
- 7 Wang Wei, Guo S., Chang Nan, Yang Wei. Optimum buckling design of composite stiffened panels using ant colony algorithm. *Compos Struct* 2010;**92**(3):712–9. Doi: 10.1016/j.compstruct.2009.09.018.

- 8 Walker M., Smith R.E. A technique for the multiobjective optimisation of laminated composite structures using genetic algorithms and finite element analysis. *Compos Struct* 2003;**62**(1):123–8. Doi: 10.1016/S0263-8223(03)00098-9.
- 9 Deveci H Arda, Aydin Levent, Seçil Artem H. Buckling optimization of composite laminates using a hybrid algorithm under Puck failure criterion constraint. *J Reinf Plast Compos* 2016;**35**(16):1233–47. Doi: 10.1177/0731684416646860.
- 10 Aydin Levent, Artem H. Secil. Comparison of stochastic search optimization algorithms for the laminated composites under mechanical and hygrothermal loadings. *J Reinf Plast Compos* 2011;**30**(14):1197–212. Doi: 10.1177/0731684411415138.
- 11 Kemal Apalak M., Yildirim Mustafa, Ekici Recep. Layer optimisation for maximum fundamental frequency of laminated composite plates for different edge conditions. *Compos Sci Technol* 2008;**68**(2):537–50. Doi: 10.1016/j.compscitech.2007.06.031.
- 12 CHANG Liang, NIE Xiaohua, LUO Lilong, et al. The isogenic sequence double random genetic algorithm used in composite ply optimizations[J]. *Advances in Aeronautical Science and Engineering*, 2023, 14(5): 70-77.
- 13 Franco Correia V. M., Mota Soares C. M., Mota Soares C. A. DESIGN SENSITIVITY ANALYSIS AND OPTIMAL DESIGN OF COMPOSITE STRUCTURES USING HIGHER ORDER DISCRETE MODELS. *Eng Optim* 1997;**29**(1–4):85–111. Doi: 10.1080/03052159708940988.
- 14 Khot N. S., Venkayya V. B., Berke L. Optimum Design of Composite Structures with Stress and Displacement Constraints. *AIAA J* 1976;**14**(2):131–2. Doi: 10.2514/3.61345.
- 15 Bruyneel M, Fleury C. Composite structures optimization using sequential convex programming. *Adv Eng Softw* 2002.
- 16 Harte A.M., McNamara J.F., Roddy I. Evaluation of optimisation techniques in the design of composite pipelines. *J Mater Process Technol* 2001;**118**(1–3):478–84. Doi: 10.1016/S09240136(01)00989-X.
- 17 Topal Umut, Uzman Ümit. Maximization of buckling load of laminated composite plates with central circular holes using MFD method. *Struct Multidiscip Optim* 2008;**35**(2):131–9. Doi: 10.1007/s00158-007-0119-1.
- 18 Sørensen René, Lund Erik. Thickness filters for gradient based multi-material and thickness optimization of laminated composite structures. *Struct Multidiscip Optim* 2015;**52**(2):227–50. Doi: 10.1007/s00158-015-1230-3.
- 19 Henriksen Søren R., Weaver Paul M., Lindgaard Esben, Lund Erik. Post-buckling optimization of composite structures using Koiter's method. *Int J Numer Methods Eng* 2016;**108**(8):902–40. Doi: 10.1002/nme.5239.
- 20 Gao Tong, Zhang Weihong. A mass constraint formulation for structural topology optimization with multiphase materials. *Int J Numer Methods Eng* 2011;**88**(8):774–96. Doi: 10.1002/nme.3197.
- 21 Stegmann J., Lund E. Discrete material optimization of general composite shell structures: DISCRETE MATERIAL OPTIMIZATION OF GENERAL COMPOSITE SHELL STRUCTURES. *Int J Numer Methods Eng* 2005;**62**(14):2009–27. Doi: 10.1002/nme.1259.
- 22 Duan Zunyi, Yan Jun, Zhao Guozhong. Integrated optimization of the material and structure of composites based on the Heaviside penalization of discrete material model. *Struct Multidiscip Optim* 2015;**51**(3):721–32. Doi: 10.1007/s00158-014-1168-x.
- 23 Sci-Hub | On design of fiber-nets and orientation for eigenfrequency optimization of plates

- | 10.1007/s00466-005-0002-0. Available at <https://sci-hub.et-fine.com/10.1007/s00466-0050002-0>. Accessed October 16, 2023, n.d.
- 24 Niu Bin, Shan Yao, Lund Erik. Discrete material optimization of vibrating composite plate and attached piezoelectric fiber composite patch. *Struct Multidiscip Optim* 2019;**60**(5):1759–82. Doi: 10.1007/s00158-019-02359-8.
 - 25 Bruyneel Michael. SFP—a new parameterization based on shape functions for optimal material selection: application to conventional composite plies. *Struct Multidiscip Optim* 2011;**43**(1):17–27. Doi: 10.1007/s00158-010-0548-0.
 - 26 Gao Tong, Zhang Weihong, Duysinx Pierre. A bi-value coding parameterization scheme for the discrete optimal orientation design of the composite laminate: BCP SCHEME FOR THE DISCRETE OPTIMAL ORIENTATION DESIGN OF THE LAMINATE. *Int J Numer Methods Eng* 2012;**91**(1):98–114. Doi: 10.1002/nme.4270.
 - 27 Luo Yunfeng, Chen Wenjiong, Liu Shutian, Li Quhao, Ma Yaohui. A discrete-continuous parameterization (DCP) for concurrent optimization of structural topologies and continuous material orientations. *Compos Struct* 2020;**236**:111900. Doi: 10.1016/j.compstruct.2020.111900.
 - 28 Zhang Lanting, Guo Laifu, Sun Pengwen, Yan Jinshun, Long Kai. A generalized discrete fiber angle optimization method for composite structures: Bipartite interpolation optimization. *Int J Numer Methods Eng* 2022;nme.7160. Doi: 10.1002/nme.7160.
 - 29 Yan Jun, Duan Zunyi, Lund Erik, Wang Jingyuan. Concurrent multi-scale design optimization of composite frames with manufacturing constraints. *Struct Multidiscip Optim* 2017;**56**(3):519–33. Doi: 10.1007/s00158-017-1750-0.
 - 30 Niu Michael Chun-Yung. *Airframe structural design: practical design information and data on aircraft structures*. 2. ed., 3. publ. with minor corr. Hong Kong: Conmilit Press Ltd; 2006.
 - 31 Herencia J. Enrique, Weaver Paul M., Friswell Michael I. Optimization of Long Anisotropic Laminated Fiber Composite Panels with T-Shaped Stiffeners. *AIAA J* 2007;**45**(10):2497–509. Doi: 10.2514/1.26321.
 - 32 Liu Xiaoyang, Featherston Carol A., Kennedy David. Two-level layup optimization of composite laminate using lamination parameters. *Compos Struct* 2019;**211**:337–50. Doi: 10.1016/j.compstruct.2018.12.054.
 - 33 Fedon Noémie, Weaver Paul M., Pirrera Alberto, Macquart Terence. A repair algorithm for composite laminates to satisfy lay-up design guidelines. *Compos Struct* 2021;**259**:113448. Doi: 10.1016/j.compstruct.2020.113448.
 - 34 Liu Dianzi, Toropov Vassili V., Querin Osvaldo M., Barton David C. Bilevel Optimization of Blended Composite Wing Panels. *J Aircr* 2011;**48**(1):107–18. Doi: 10.2514/1.C000261.
 - 35 Bruyneel Michael, Beghin Clément, Craveur Guillaume, Grihon Stéphane, Sosonkina Masha. Stacking sequence optimization for constant stiffness laminates based on a continuous optimization approach. *Struct Multidiscip Optim* 2012;**46**(6):783–94. Doi: 10.1007/s00158012-0806-4.
 - 36 Tsai Stephen W. Double–Double: New Family of Composite Laminates. *AIAA J* 2021;**59**(11):4293–305. Doi: 10.2514/1.J060659.
 - 37 Shrivastava Sachin, Sharma Naresh, Tsai Stephen W., Mohite P.M. D and DD-drop layup optimization of aircraft wing panels under multi-load case design environment. *Compos Struct* 2020;**248**:112518. Doi: 10.1016/j.compstruct.2020.112518.

- 38 Zhao Kai, Kennedy David, Miravete Antonio, Tsai Stephen W., Featherston Carol A., Liu Xiaoyang. Defining the Design Space for Double–Double Laminates by Considering Homogenization Criterion. *AIAA J* 2023;1–14. Doi: 10.2514/1.J062639.
- 39 Vermes Bruno, Tsai Stephen W., Massard Thierry, Springer George S., Czigany Tibor. Design of laminates by a novel “double–double” layup. *Thin-Walled Struct* 2021;**165**:107954. Doi: 10.1016/j.tws.2021.107954.
- 40 Kappel Erik. Double–Double laminates for aerospace applications — Finding best laminates for given load sets. *Compos Part C Open Access* 2022;**8**:100244. Doi: 10.1016/j.jcomc.2022.100244.
- 41 Wang Yan, Wang Dan, Zhong Yucheng, Rosen David W., Li Shuxin, Tsai Stephen W. Topology optimization of Double-Double (DD) composite laminates considering stress control. *Comput Methods Appl Mech Eng* 2023;**414**:116191. Doi: 10.1016/j.cma.2023.116191.
- 42 Tsai Stephen W. Expectation of the next generation research in composite materials 2023. 43 Song Longlong, Zhao Jian, Gao Tong, Li Jiajia, Tang Lei, Li Yang, et al. Length scale control in density-based multi-material topology optimization. *Comput Methods Appl Mech Eng* 2022;**401**:115655. Doi: 10.1016/j.cma.2022.115655.